



Effect of El Niño on the response ratio of Hadley circulation to different SST meridional structures

Juan Feng¹ · Jianping Li^{1,2} · Fei-Fei Jin³ · Zhengyu Liu⁴ · Sen Zhao³

Received: 11 September 2018 / Accepted: 1 April 2019 / Published online: 16 April 2019
© The Author(s) 2019

Abstract

The role of El Niño in influencing the response of the Hadley circulation (HC) to different tropical sea surface temperature (SST) meridional structures is investigated over the period 1979–2016. The explained variance of the equatorially asymmetric principal mode of HC variability is enhanced during El Niño events that are characterized by equatorially symmetric El Niño SST anomalies. It is shown that the response of the HC to different SST meridional structures is greatly enhanced in El Niño events; this is because the SST over the Indo-Pacific warm pool (IPWP) shows inhomogeneous warming in El Niño events, with greater values in the southern IPWP. The asymmetric warming over the IPWP is opposite to the climatological meridional structure of the SST over the IPWP, which intensifies the equatorially symmetric variation of SST, and contributes to the enhanced response of the HC to SST. This point is further verified by the suppression of this enhanced response in El Niño events of the HC to SST when the effects of SST over the IPWP are removed, implying that the different warming amplitude within the IPWP during the El Niño events contributes to the enhanced response. The response in La Niña events is also explored, indicating a difference between El Niño and La Niña events. These results may help explain the corresponding variations of the HC during the El Niño events, and highlight the different influences of the El Niño and La Niña events on the response of the HC to SST.

Keywords Hadley circulation · Sea surface temperature · Equatorially asymmetric · Equatorially symmetric · Indo-Pacific warm pool

1 Introduction

The El Niño/Southern Oscillation (ENSO) phenomenon is the most significant interannual climate signal in the tropical atmosphere–ocean interaction, and has widespread impacts on the global climate system and socio-economic activity.

There has been extensive research into its dynamics (e.g., Bjerknes 1969; Cane and Zebiak 1985; Picaut et al. 1997), interannual variations (e.g., Jin 1997a, b; Wang et al. 1999; Latif and Keenlyside 2008), decadal variability (e.g., Latif et al. 1997; Zhang et al. 1997), and regional impacts (e.g., Nicholls 1979; Kiladis and Diaz 1989; Tomita and Yasunari 1996; Wang et al. 2000; Xie et al. 2009; Feng and Li 2011). Among these, the influence of ENSO on the Hadley circulation (HC) has attracted wide interest because the HC is a thermally driven meridional circulation and is sensitive to changes in the underlying thermal conditions (Fu et al. 2006; Mitas and Clement 2006; Hu and Fu 2007; Lu et al. 2008, 2009). Intensified subtropical jets and HC have been observed during El Niño events (Seager et al. 2003), and the relationship between the boreal winter HC and El Niño has been considered (e.g., Mitas and Clement 2005; Stachnik and Schumacher 2011). The possible connection between El Niño and the long term variability of seasonal HC were investigated (Ma and Li 2008; Feng et al. 2011; Sun and Zhou 2014; Guo et al. 2016). Meanwhile, it has

✉ Juan Feng
fengjuan@bnu.edu.cn

¹ College of Global Change and Earth System Science (GCESS), Beijing Normal University, Beijing, China

² Key Laboratory of Physical Oceanography–Institute for Advanced Ocean Studies, Ocean University of China, Qingdao National Laboratory for Marine Science and Technology, Qingdao, China

³ School of Ocean and Earth Science and Technology, University of Hawaii at Manoa, Honolulu, HI, USA

⁴ Atmospheric Science Program, Department of Geography, Ohio State University, 154 N. Oval Mall, Columbus, OH, USA

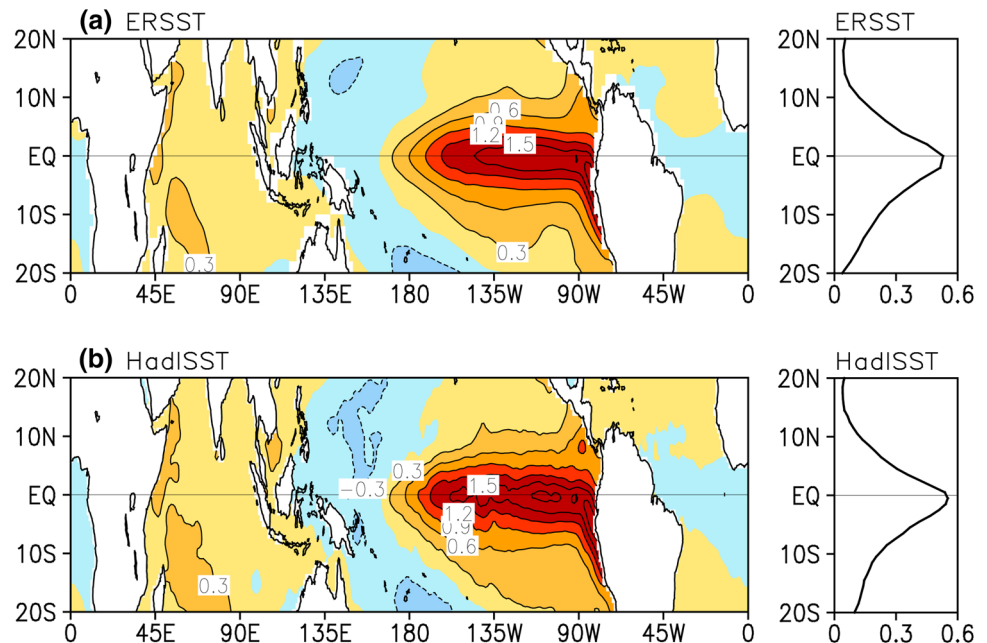
been demonstrated that the sea surface temperature (SST) over the Indo-Pacific warm pool (IPWP) plays an important role in determining the interdecadal variation of the HC (e.g., Ma and Li 2008; Feng et al. 2011; Li and Feng 2017). The continuous warming of the IPWP favours the intensification of the boreal spring and winter HC (Li and Feng 2017). These studies show that the SST over both the IPWP and tropical Pacific has an important impact on the variations of the HC.

In addition, previous studies have found that the meridional distribution of tropical SST has an important influence on the spatial and temporal variations of the HC. For example, earlier theoretical studies have indicated that the strength and position of the convergence (Schneider and Lindzen 1977; Rind and Rossow 1984), as well as the vertical motion (Lindzen and Nigam 1987; Hou and Lindzen 1992) in the lower levels are altered by the adjustment of the meridional structure of the underlying tropical SST. Results from Numaguti (1994) further support this viewpoint, that the meridional gradient of tropical SST has a strong influence on the convergence in the planetary boundary layer. Our previous studies based on theoretical and observational analysis have illustrated that the meridional structure of tropical SST determines the spatial distribution of the HC (Feng and Li 2013; Li and Feng 2017). The position of ascent of the HC adjusts to the position where the meridional gradient of SST equals zero and its value is changing from positive to negative (Feng and Li 2013). That is, an equatorially symmetric (asymmetric) anomalous meridional circulation is accompanied by an equatorially symmetric (asymmetric) anomalous SST forcing. For example, intensified inhomogeneous warming over the IPWP alters the meridional gradient

of tropical SST, which in turn contributes to the formation and trend of the long-term variability of the HC (Li and Feng 2017). Besides the qualitative influence of the meridional distribution of SST on the HC, it has been demonstrated that the amplitude of the HC response to equatorially asymmetric SST is approximately five times as strong as that to the equatorially symmetric SST on interannual timescales (Feng et al. 2016), and it is about four times as strong in the seasonal cycle (Feng et al. 2017). These studies quantitatively emphasize the important role of the meridional structure of SST on the HC over interannual and seasonal timescales, in the context of the response of the HC to SST under general climatological conditions.

However, ENSO shows not only strong difference in the SST anomaly zonal structure, but also exhibits evident meridional structure in both its warm and cold events (Zhang et al. 2009, 2013). In general, an El Niño event is associated with an equatorially symmetric SST structure (i.e., with the maximum SST anomalies around the equator), as shown in Fig. 1. Does the occurrence of El Niño events alter the meridional structure of tropical SST? In an earlier paper we reported that an anomalous equatorially symmetric meridional circulation (i.e., with the maximum anomalous ascent around the equator; Feng and Li 2013) is related to El Niño events during boreal spring. Does the spatial distribution of the meridional circulation change during the evolution of El Niño events? Moreover, if the occurrence of El Niño events alters the meridional structure of tropical SST, does the sensitivity of the HC to the meridional distribution of the SST (Feng et al. 2016, 2017) change the response of the HC to SST? Therefore, it is of interest to examine whether and to what extent the

Fig. 1 **a** Spatial SST anomalies during the six El Niño events (1982/1983, 1986/1987, 1991/1992, 1997/1998, 2009/2010, and 2015/2016) and their globally zonal-mean profile based on ERSST ($^{\circ}$ C). **b** As in **a**, but based on HadISST



meridional structures of the SST are changed, and in turn whether the amplitudes of the response of the HC to SST are altered during the El Niño events. Accordingly, one of the key goals of the present study is to quantitatively investigate and compare the differences in the response of the HC to SST during the El Niño cases and over the whole study period, and to explore the role of El Niño events in the variation of the HC.

To compare the impact of El Niño on the amplitude of the response of the HC to SST, the variations of the HC and tropical SST are linearly separated into two components (i.e., equatorially asymmetric and symmetric) to explore the corresponding variations in their response ratio during the El Niño events and in the whole study period following Feng et al. (2017). The remainder of this paper is organized as follows. Section 2 describes the datasets and methodology. The variations of the response ratio of the HC to different SST meridional structures during the El Niño events are shown in Sect. 3. Section 4 describes the possible reasons for these different response contrasts. The possible situation during the La Niña events is discussed in Sect. 5. Finally, Sect. 6 contains a short discussion and our conclusions.

2 Datasets and methodology

2.1 Datasets

Two global SST datasets were used to estimate the possible role of El Niño in determining the response of the HC to tropical SST. These widely used datasets were the Extended Reconstructed SST version 3 on a $2^\circ \times 2^\circ$ grid (ERSST; Smith et al. 2008), and the UK Met Office Hadley Centre's sea ice and SST dataset with $1^\circ \times 1^\circ$ resolution (HadISST; Rayner et al. 2003). The Niño 3 index is used to identify El Niño and La Niña events (areal averaged SST over 5°S – 5°N , 150°W – 90°W) available via https://www.esrl.noaa.gov/psd/gcos_wgsp/Timeseries/Data/nino3.long.anom.data. Three atmospheric reanalysis datasets were used to obtain the characteristics of HC: the European Centre for Medium-Range Weather Forecasts (ECMWF) Re-Analysis interim (ERA1) globally archived dataset that covers 1979 to 2016 with a resolution of $1.5^\circ \times 1.5^\circ$ on 32 vertical levels (Dee et al. 2011), the Japanese 55-year Reanalysis dataset (JRA) that covers 1979–2016 on a resolution of $1.25^\circ \times 1.25^\circ$ and 32 vertical levels (Ebita et al. 2011), and the National Centers for Environmental Prediction–Department of Energy Atmospheric Model Intercomparison Project reanalysis (NCEP2) covering the period 1979–2016 on 17 vertical levels (Kanamitsu et al. 2002). Multi-reanalyses were used to verify the reliability of the results. Here, the common available period

of 1979–2016 was used as the climatological mean, and the annual cycle was removed before the analyses.

2.2 Method

To illustrate the role of El Niño in determining the response contrast of the HC to SST, instead of the calendar year we consider an austral year that depicts a whole cycle of an El Niño event; i.e., from July of 1 year to the following June. The austral year in which the monthly Niño 3 index is above (below) 0.5°C (-0.5°C) for at least 9 months is defined as an El Niño (La Niña) event. This gives six El Niño events (i.e., 1982/1983, 1986/1987, 1991/1992, 1997/1998, 2009/2010, and 2015/2016) and six La Niña events (i.e., 1984/1985, 1988/1989, 1998/1999, 1999/2000, 2007/2008, and 2010/2011) during the period 1979–2016. These events are consistent with the occurrence of El Niño and La Niña events in the previous studies (e.g., Zhang et al. 2015). These six warm and six cold events constitute the subsets of El Niño and La Niña events each with length of 72 (6×12) months, and the 37 reconstructed austral years (i.e., from July 1979 to June 2016) in the period 1979–2016 constitute the whole study period with a length of 444 (37×12) months in the following analysis. In addition, 12 neutral events (i.e., 1979/1980, 1981/1982, 1985/1986, 1989/1990, 1992/1993, 1996/1997, 2001/2002, 2003/2004, 2005/2006, 2008/2009, 2012/2013, and 2013/2014) are chosen that have monthly Niño 3 index in the range -0.5°C to 0.5°C for at least 9 months, to highlight the robustness of the result. Note that the result based on a subset of 6 neutral events is consistent with that based on 12 events, thus only the result based on 12 neutral events is shown here.

The HC is inferred from the mass stream-function (MSF), with the MSF exhibiting a clockwise circulation in the Northern Hemisphere (NH) and an anti-clockwise circulation in the Southern Hemisphere (SH; Holton 1994). To examine the possible impacts of El Niño events on the response of the HC to different meridional structures of tropical SST, the spatial variations in the HC and SST were separated into two components following Feng et al. (2017); i.e., the equatorially asymmetric component and the equatorially symmetric component. Note that the decomposition method was first introduced by Guan et al. (1994) and Wang et al. (1994), in which they called 'odd' (corresponding to the asymmetric variation) and 'even' (corresponding to the symmetric variation) components. Based on the decomposition, the climatic features and temporal evolution of circulations (i.e., temperature, zonal and meridional wind, geopotential height) are analysed. And they have illustrated that there is a relationship between a major El Niño event and the component anomalies. However, they did not apply this decomposition into the vertical direction, neither nor the linkage between the HC and

tropical SST. The zonal-mean SST is decomposed into the equatorially symmetric (SES) and asymmetric (SEA) variations as follows:

$$SES(y) = \frac{SST(y) + SST(-y)}{2}, \quad SEA(y) = \frac{SST(y) - SST(-y)}{2}, \quad (1)$$

where y is the meridional distance north of the equator. We define the MSF to be (a) symmetric depending on whether the vertical velocity is (a) symmetric about the equator,

$$HES(y) = \frac{MSF(y) - MSF(-y)}{2}, \quad HEA(y) = \frac{MSF(y) + MSF(-y)}{2}. \quad (2)$$

Note that the sum of the equatorially asymmetric and symmetric variations is equal to the original variations. The definitions of HEA (HES) and SEA (SES) are opposite because the vertical velocity is defined to be symmetric. More details regarding the calculation and physics of the decomposition are given in Feng et al. (2017). Note that the variations of the HEA and HES are not orthogonal, and the relationship between the HEA and HES is changeable in different seasons (Feng et al. 2018). The monthly variations of the HEA, HES, SEA and SES were obtained using the above decomposition method, and then empirical orthogonal function (EOF) analysis was used to detect the principal mode and principal component (PC) of their monthly variations. However, a global integral was used to present the temporal variation of the variables instead of the EOF in Guan et al. (1994) and Wang et al. (1994). The EOF is employed for the following considerations, i.e., the air-sea interactions in the tropics and extra-tropics are different, and it is reported the tropical SST plays important role in determining the variation of HC for which is a thermally driven circulation. The global integral method introduced in Guan et al. (1994) considers the impacts from both the tropics and extra-tropics rather than those only from the tropics. Moreover, it is seen the first dominant modes for both the tropical SST and HC explain a large portion of variances, representing their fundamental variations.

A response contrast index of the HC to different SST meridional structures is correspondingly defined as,

$$ratio = \frac{PC1(HEA)/PC1(SEA)}{PC1(HES)/PC1(SES)}, \quad (3)$$

where PC1(HEA) refers to the first PC of the variability of HEA, and similarly for other variables. The numerator (denominator) in Eq. (3) (referred as *RegA* (*RegS*)) represents the amplitude of the response of the equatorially asymmetric (symmetric) circulation to the equatorially asymmetric (symmetric) SST forcing. Thus, the index in Eq. (3) demonstrates the sensitivity of the HC to different SST meridional structures; i.e., a larger value implies a more sensitive response of the HC to the equatorially asymmetric

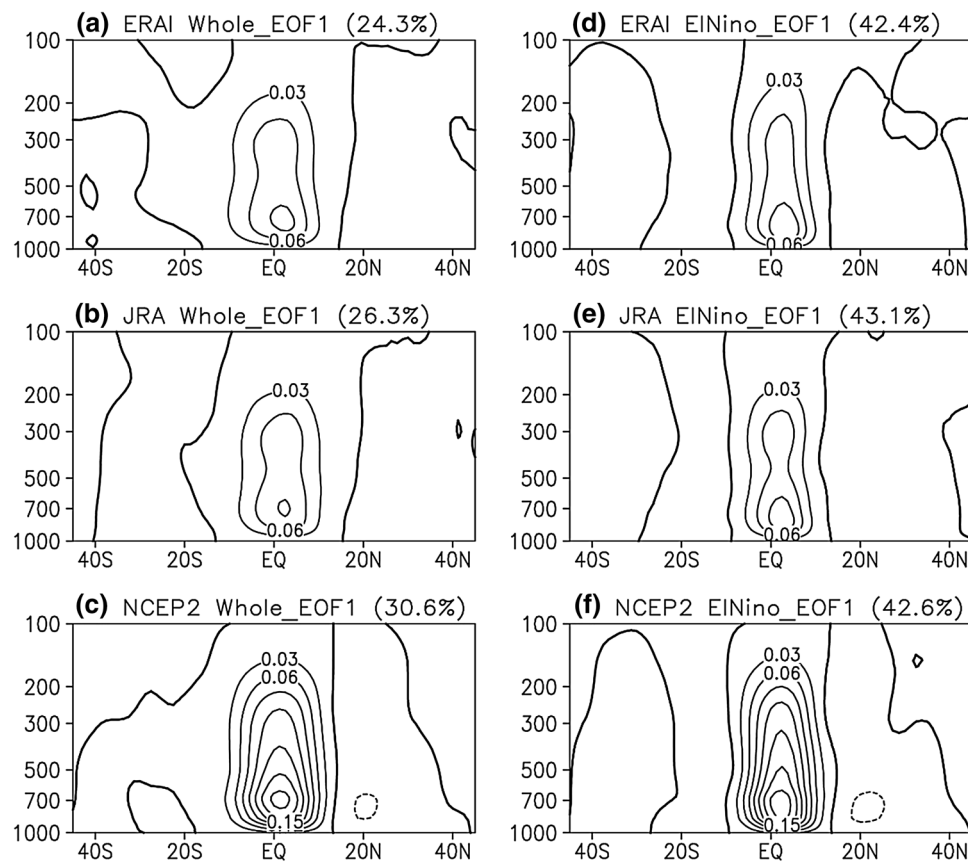
SST forcing. If the response amplitudes of the anomalous HC to the equatorially asymmetric and symmetric SST is same, then *ratio* equals to 1. Note that the decomposition here is not only a mathematical construct, it has physical meaning; for example, an El Niño-like SST pattern within the tropical Pacific generally corresponds to an equatorially symmetric SST structure as seen below. However, an SST pattern within the Atlantic related to the Atlantic Multidecadal Oscillation is equivalent to an equatorially asymmetric SST structure (Feng et al. 2018). The relationship between the HC and SST is investigated using correlation and regression analysis. The influence of the SST over the IPWP on the HC (SST) is removed by subtracting the linear regression of the HC (SST) on the SST over the IPWP, and the unrelated residual (non-IPWP variability) is the variation independent of the SST over the IPWP following Caballero (2007). The decomposition is then applied to the residuals of the HC and SST, and calculation of the response is repeated to detect the possible impacts of SST over the IPWP on the response of the HC to SST. The statistical significance of the correlation and regression values was evaluated by a two-sided Student's *t* test.

3 Impact of El Niño on the response of the HC to SST

3.1 Variations of the HC during the El Niño events

El Niño events are associated with strong positive SST anomalies within the tropical central, eastern Pacific and Indian ocean (Kumar and Hoerling 2003), and relatively weak negative SST anomalies over the western Pacific (DeWeaver and Nigam 2004), with maximum amplitudes around the equator, decreasing poleward gradually (Fig. 1); this results in an overall basin-wide zonally averaged heating over the tropical Pacific Ocean that displays a sinusoidal-like meridional distribution with the maximum around the equator. Thus, an equatorially symmetric SST anomaly pattern accompanies the El Niño events. The corresponding global mean anomalous meridional circulation is shown in Fig. 2. Considering the interannual variability of the HC over the whole study period, the first dominant mode of the anomalous HC (EOF1) is equatorially asymmetric; i.e., with the combined ascending branch located to the south of the equator, and descent around 15°N. This mode is consistently observed in the three atmospheric reanalyses, explaining a variance of ~25%. Note that the spatial distribution of this mode is similar to that of the long term seasonal variability (Ma and Li 2008; Li and Feng 2017) and annual cycle (Dima and Wallace 2003; Feng et al. 2017) of the HC, but with smaller explained variance. An equatorially asymmetric mode with similar intensity (the maximum values of MSF)

Fig. 2 Left panel: EOF1 of the monthly MSF during the whole study period 1979–2016 based on **a** ERAI, **b** JRA, and **c** NCEP2. The contour interval is $0.03 \times 10^{10} \text{ kg s}^{-1}$. Solid (dotted) contours are positive (negative) and the zero contour is thickened. Right panel: as in left panel, but during the El Niño events



and extent (defined by the differences between the locations of the ascending and descending branch) is observed during the El Niño events. However, the explained variance of this mode is evidently enhanced during the El Niño events compared with the whole period (above 40% in the subset of El Niño events). The enhanced explained variance of the equatorially asymmetric mode of the HC is found across the three reanalyses, indicating its robustness. In addition, we examine whether the length of the sample influences the explained variance in EOF analysis. To verify the possible influence of the sample length, the EOF results during the six La Niña events (the sample length is same as that during the El Niño events) and 12 neutral events (the sample length is larger as that during the El Niño events) are chosen to give a direct comparison. It is consistently observed in both ERAI and JRA reanalyses (not shown) that the explained variance for the first dominant mode of the HC during the La Niña events (with ~24% explained variance) and neutral events (with ~23% explained variance) is comparable to that over the whole period (with ~24% explained variance). This result suggests that the enhanced explained variance of the equatorially asymmetric mode of the HC during the El Niño events is not due to the smaller sample.

The enhanced explained variance of the asymmetric mode does not follow directly from the conclusion in Feng and Li

(2013) that an equatorially symmetric anomalous SST is associated with an equatorially symmetric meridional circulation. The possible reason why an increased (rather than suppressed) explained variance of the equatorially asymmetric circulation is observed during the El Niño events is discussed below.

3.2 Enhanced response ratio of the HC to SST during the El Niño events

To explore the possible causes of the enhanced explained variance of the equatorially asymmetric mode during the El Niño events, we first decompose the variations of the tropical zonal-mean SST into the SEA and SES components, to analyze their separate variations during the El Niño events. The principal modes of the SEA and SES in the whole study period and during the El Niño events are shown in Fig. 3. A sinusoidal-like distribution dominates the variations of SEA over both the whole period and El Niño event cases. In contrast, the dominant mode of SES is a Gaussian distribution, with the maximum at the equator. Note that differences between the El Niño events and the whole period are small, in both the spatial distribution of the first dominant mode of both SEA and SES, and the explained variances of the

Fig. 3 **a** EOF1 of the equatorially asymmetric variation of SST over the whole study period. Red (blue) lines indicate based on ERSST (HadISST) data with the corresponding explained variance in brackets. **b** As in **a**, but for the equatorially symmetric variation of SST. **c, d** As in **a, b**, but during the El Niño events

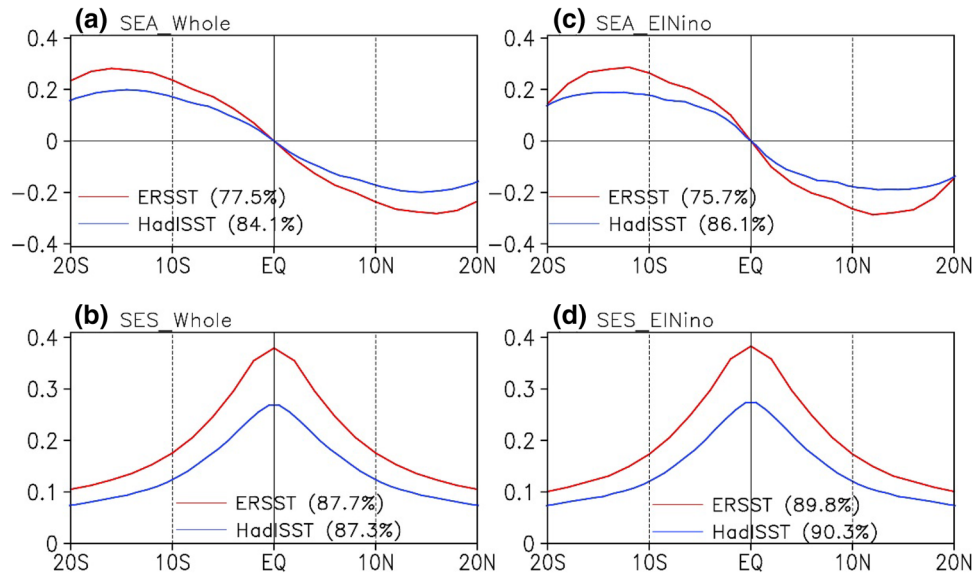
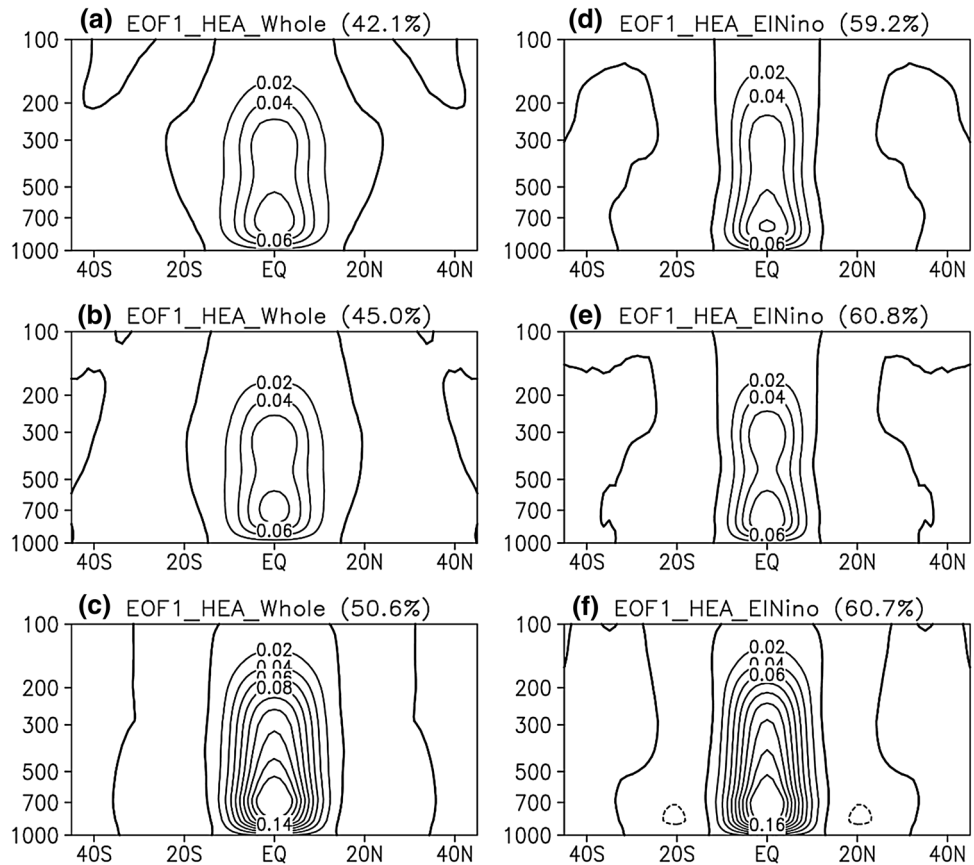


Fig. 4 Left panel: EOF1 of the equatorially asymmetric variation of the HC during the whole study period based on **a** ERAI, **b** JRA, and **c** NCEP2 reanalyses. The contour interval is $0.02 \times 10^{10} \text{ kg s}^{-1}$. Solid (dotted) contours are positive (negative) and the zero contour is thickened. Right panel: As in left panel, but during the El Niño events



dominant modes for both the SEA (i.e., changes are less than 2%) and SES (i.e., changes are less than 3%).

The principal mode of variation of the HEA and the HES over the whole period is shown in Fig. 4. The EOF1 of HEA is dominated by an equatorially asymmetric cell, explaining a variance of $\sim 45\%$ across the different reanalyses, with

ascending and descending branches around 15°S and 15°N , respectively. The extent, intensity, and explained variance of this mode are consistent across the three reanalyses. Note that the spatial distribution of this mode resembles that of the total HC as shown in Fig. 2 (left panel). A similar spatial structure of the EOF1 is observed during the El Niño events,

but with evident enhanced explained variance ($\sim 60\%$), which agrees well in different reanalyses. This result implies that the EOF1 of HEA is more concentrated during the El Niño events, supporting the result that the variance explained by the equatorially asymmetric mode is increased during the El Niño events (compare right panels in Figs. 2 and 4). Note that the explained variance ($\sim 40\%$) of the first dominant mode of the HEA during the La Niña events and neutral events is comparable to that over the whole period (not shown), confirming that the enhanced explained variance of the dominant mode for HEA during the El Niño events is not due to the smaller sample.

As for the variability of the HES, we see that its EOF1 displays an equatorially symmetric structure, explaining about 40% of the variance (Fig. 5). The combined ascending branch of this mode is located at the equator, and the two descending branches are located at about 30° latitude in both hemispheres. As with the HEA, the explained variance of this mode is enhanced during the El Niño events ($\sim 50\%$ vs. $\sim 40\%$). Although the spatial distributions of the dominant modes of HEA and HES during the El Niño events are not very different from those in the whole period, the explained variances are substantially enhanced, unlike the zonal-mean SST that has similar explained variances for the dominant modes of SEA and SES during the El Niño events to those

for the whole study period. This result implies that there may a change in the response of the HC to SST or that the changes in the explained variances of HC and SST are not equivalent, particularly for that in the HEA. We therefore compare the response of the HC to different SST meridional structures in the whole period and during the El Niño events.

Figure 6 presents scatterplots of the first PC1 of SEA versus HEA, and for the first PC of SES versus HES during both the whole period and for El Niño events. Here SST is from ERSST and the MSF is calculated from ERAI. It is clear that HES and SES are significantly correlated with each other, as are HEA and SEA. Note that the relationship between the PC1s of HEA (HES) and SES (SEA) is insignificant during both the whole period and El Niño events (not shown), which is consistent with previous work (Feng et al. 2016, 2017). Moreover, the response amplitude of HEA to SEA is much larger than that of HES to SES (Fig. 6; Table 1). The response of HEA to SEA is about four times that of HES to SES during the whole period. However, it is approximately ten times that of HES to SES during the El Niño events (Fig. 6). Although the regression coefficients of HEA (HES) to SEA (SES) show certain differences, the ratios of the HEA to SEA and HES to SES are comparable across different reanalyses (Table 1). More

Fig. 5 As in Fig. 4, but for the EOF1 of the equatorially symmetric variation of the HC

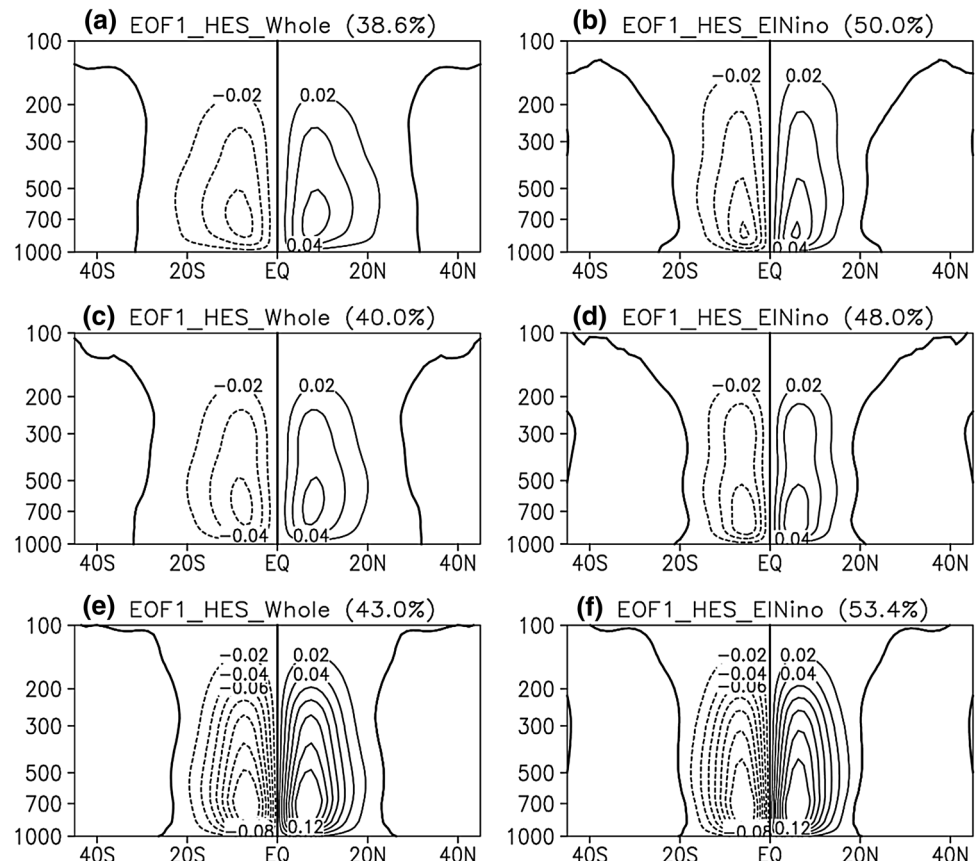


Fig. 6 **a** Scatterplot of the PC1 of the equatorially asymmetric variation of SST (from ERSST) against the PC1 of the equatorially asymmetric variation of the HC (from ERAI) (red dots), and their linear fit (black crosses) during the whole study period. **b** As in **a**, but for the equatorially symmetric variation of the SST and HC. **c, d** As in **a, b**, but during the El Niño events

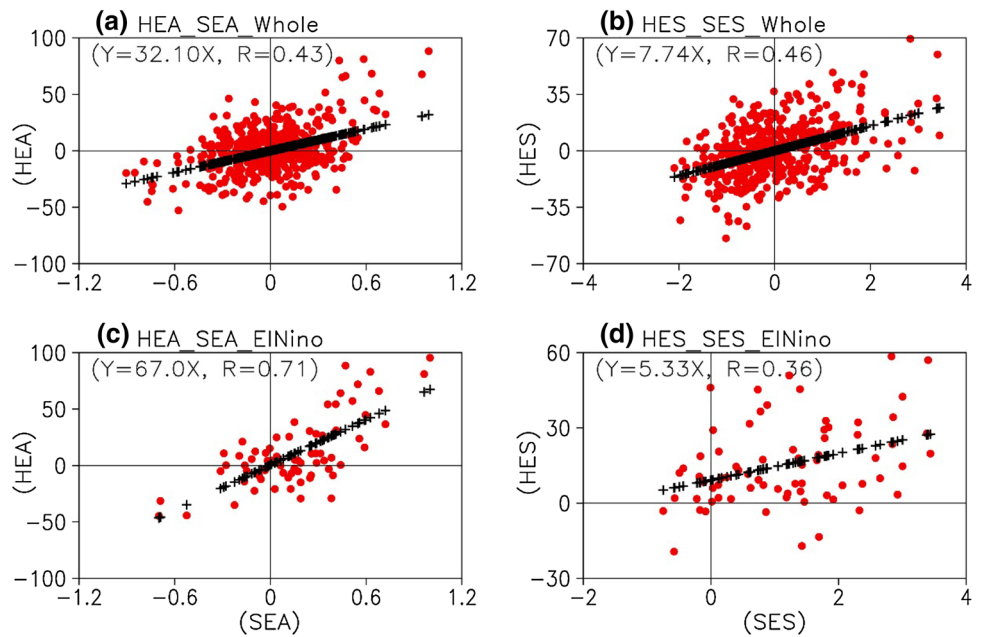


Table 1 Regression coefficients (RegA/RegS) between the HEA/HES PC1 with respect to the SEA/SES PC1 and their ratio calculated using the various reanalysis datasets

Period	Type	Raw data			Without the effects of IPWP		
		ERAI	JRA	NCEP2	ERAI	JRA	NCEP2
Whole period	RegA	32.10* (21.22*)	40.02* (25.86*)	17.39* (12.20*)	32.12* (21.20*)	40.21* (26.35*)	17.38* (11.98*)
	RA	0.43* (0.46*)	0.43* (0.45*)	0.37* (0.43*)	0.43* (0.47*)	0.44* (0.47*)	0.37* (0.42*)
	RegS	7.74* (5.28*)	12.18* (7.98*)	4.43* (3.23*)	9.07* (6.29*)	11.09* (7.41*)	6.64* (4.58*)
	RS	0.46* (0.44*)	0.58* (0.54*)	0.45* (0.47*)	0.40* (0.39*)	0.42* (0.40*)	0.50* (0.48*)
	Ratio	4.1 (4.0)	3.3 (3.2)	3.9 (3.8)	3.5 (3.4)	3.6 (3.6)	2.6 (2.6)
El Niño	RegA	67.0* (39.37*)	74.22* (41.67*)	33.34* (19.66*)	70.31* (41.50*)	80.03* (45.60*)	33.78* (19.84*)
	RA	0.71* (0.74*)	0.68* (0.67*)	0.68* (0.70*)	0.74* (0.78*)	0.73* (0.74*)	0.68* (0.71*)
	RegS	5.33* (3.78*)	11.40* (7.99*)	3.16* (2.33*)	9.79* (6.19*)	17.97* (11.27*)	5.97* (3.51*)
	RS	0.36* (0.36*)	0.62* (0.62*)	0.36* (0.38*)	0.31* (0.31*)	0.52* (0.51*)	0.34* (0.31*)
	Ratio	12.6 (10.4)	6.5 (5.2)	10.6 (8.4)	7.2 (6.7)	4.5 (4.0)	5.7 (5.7)

RA/RS are for the correlation coefficients between the HEA/HES PC1 and SEA/SES PC1. Significant coefficients at the 0.05 level are marked with asterisks. The values outside (within) the brackets are based on ERSST (HadISST)

importantly, the greater response amplitude of HEA to SEA than of HES to SES is further enhanced during the El Niño events. Note that the EOF1 amplitudes for SEA and SES are comparable (Fig. 3); a stronger response of the HC to SST during the El Niño events means that the equatorially asymmetric variations in the HC are intensified under the same magnitude of anomalous SST forcing, corresponding to the enhanced explained variances of the equatorially asymmetric mode during the El Niño events as shown in Fig. 2. However, the explained variances of the principal mode for both the SEA and SES do not

change much during the El Niño events, as they are not affected by the significant equatorially symmetric anomalous SST that accompanies El Niño. This indicates that SST variation in the tropical Pacific may not explain the enhanced response ratio of the HC to SST. Therefore, the associated variations of tropical SST in different ocean basins are further examined to illustrate the regional SST characteristics during the El Niño events.

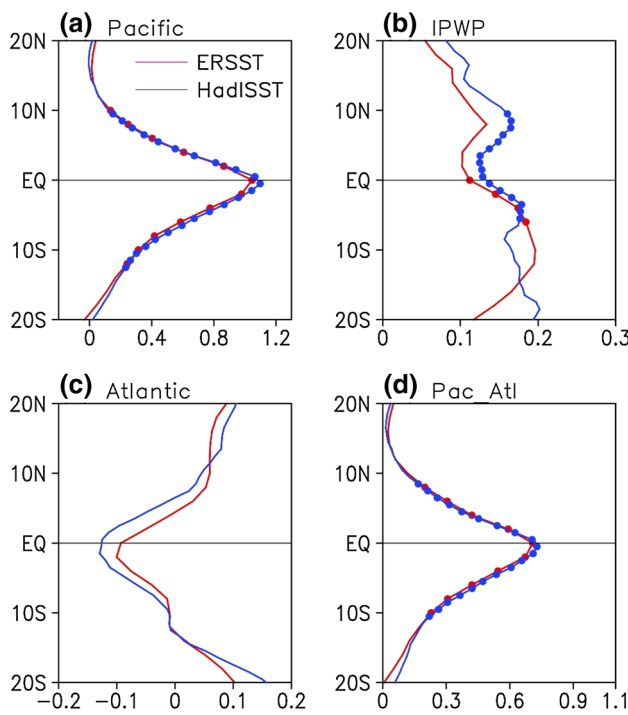


Fig. 7 Profiles of zonal-mean SST anomalies within the tropical **a** Pacific (140°E – 60°W), **b** IPWP (30°E – 140°E), **c** Atlantic (60°W – 30°E), and **d** sum of the Pacific and Atlantic (140°E – 30°E) during the El Niño events. Red (blue) lines indicate based on ERSST (HadISST) data, dotted line indicates significant at the 0.1 level

4 Role of the SST over the IPWP in the enhanced response of the HC to SST during the El Niño events

The regional SST variation in different ocean basins is displayed to further explore the meridional structures of tropical SST during the El Niño events (Fig. 7). The ERSST and HadISST data consistently show that the zonal-mean profiles of anomalous SST within the Pacific and Atlantic are equatorially symmetric with maximum magnitude at the equator during the El Niño events (Fig. 7a, c), despite having different signs (i.e., positive anomalies over the tropical Pacific, but negative over the tropical Atlantic). The variations averaged over the tropical Pacific and Atlantic are also equatorially symmetric (Fig. 7d). In contrast, the profile of zonal SST over the IPWP shows an inhomogeneous variation, with larger anomalies in the southern region of the IPWP (Kumar and Hoerling 2003; also see in Fig. 1). That is, an anomalous equatorially asymmetric SST within the IPWP develops during the El Niño events. The asymmetric variations of SST over the IPWP are further examined during the life cycle of the El Niño events. The asymmetric anomalies of tropical SST within the IPWP between the southern and northern counterparts gradually strengthen as the El Niño events develop

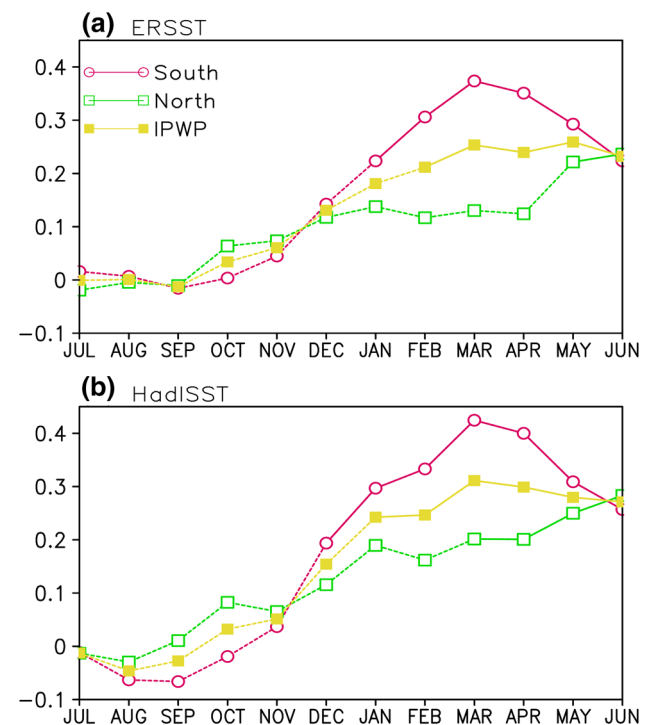


Fig. 8 **a** Seasonal cycle of the areal mean SST anomalies within the southern region (purple), northern region (green), and whole (yellow) of the IPWP during the El Niño cycle using ERSST data. **b** As in **a**, but using HadISST data. The solid line is significant at the 0.1 level

(Fig. 8), showing the largest difference in the mature and decay phases (i.e., from February to May). This suggests that El Niño events may intensify an equatorially asymmetric anomalous SST with greater values in the southern IPWP. However, the meridional structure of the anomalous warming over the IPWP during the El Niño events is opposite to its climatological SST distribution over the IPWP. The northern IPWP is warmer than the southern in the climatology; i.e., the areal mean SST over the northern (southern) IPWP is 28.5°C (27.7°C), implying that the equatorially asymmetric SST variation over the IPWP would be suppressed, resulting in strengthened equatorially symmetric SST variation during the El Niño events.

The above deduction regarding the influences of the asymmetric warming over the IPWP on the SST variability is based on the associated standard deviations of SST in the following two cases: in the raw data and after removing the effects of SST over the IPWP during the El Niño events. The standard deviation of SEA shows little change between these two cases. However, the standard deviation of SES is smaller when the effects of SST variation over the IPWP are removed (Fig. 9). Meanwhile, the variability of HEA and HES changes little after removing the effects of SST over the IPWP during the El Niño events (Fig. 10). The result indicates that the asymmetric warming over the IPWP during

Fig. 9 **a** The distribution of standard deviation of SEA during the El Niño events for the raw (red) and after removing the effects of SST over the IPWP (blue). **b** As in **a**, but for the SES. **c** The distribution of standard deviation of SEA in the whole study period (red) and during the El Niño events (blue). **d** As in **c**, but for the SES

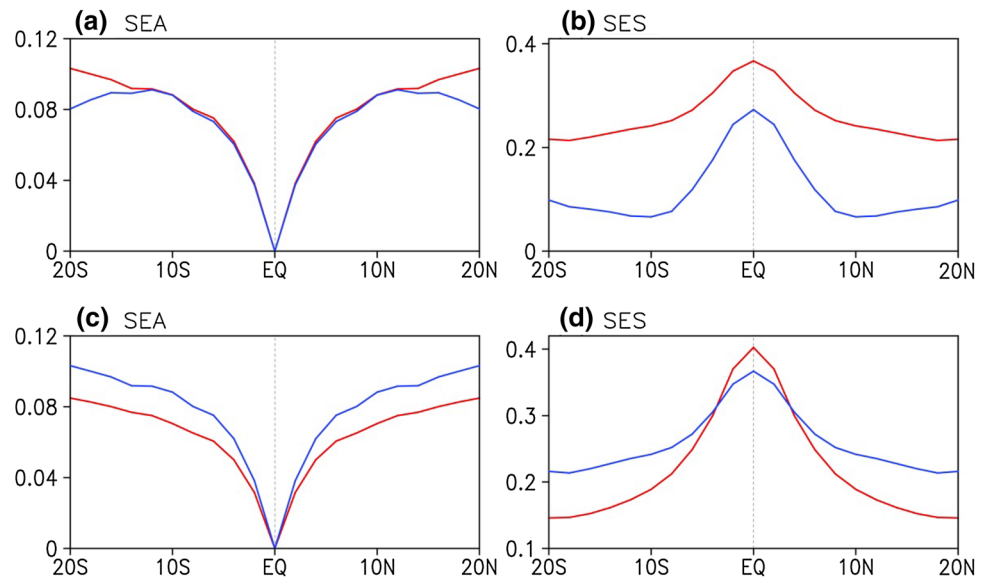
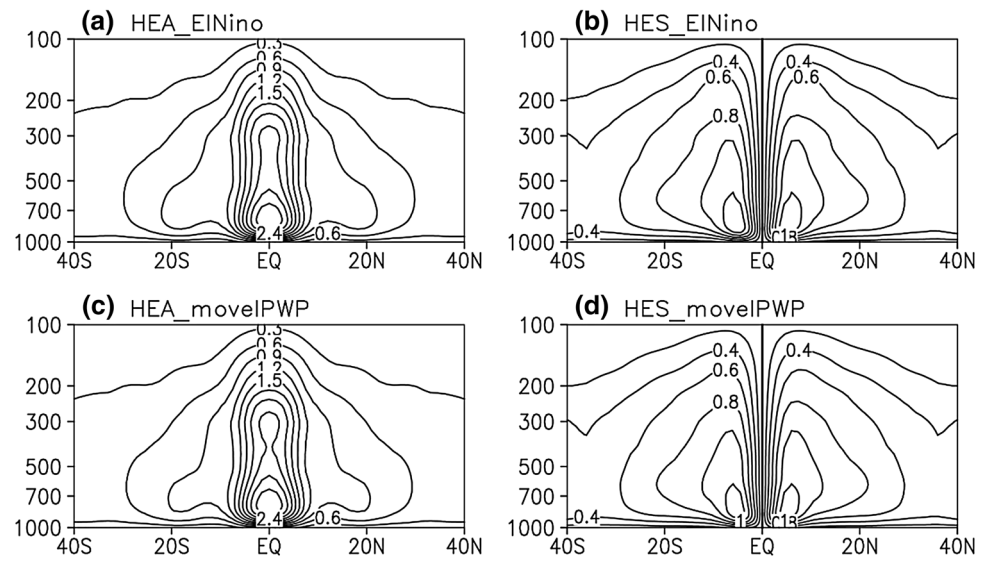


Fig. 10 **a** The distribution of standard deviation of HEA during the El Niño events. **b** As in **a**, but for the HES. **c**, **d** As in **a**, **b**, but after removing the effects of SST over the IPWP

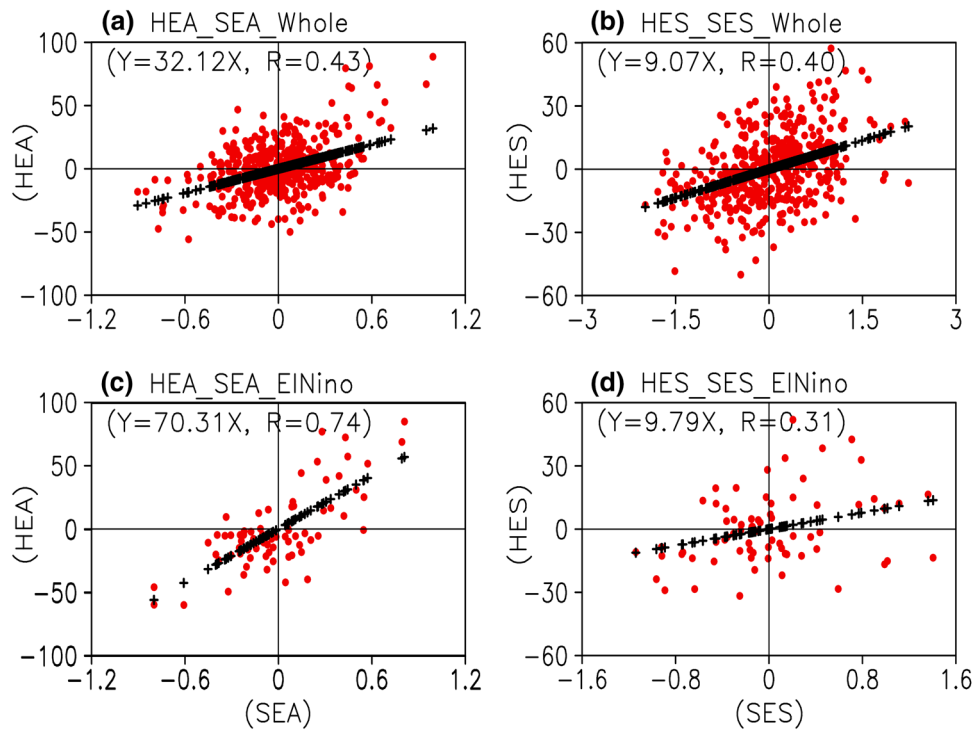


the El Niño events plays a role in influencing the response of the HC to SST by intensifying the variability of the SES.

On this point, we further verified the role of the asymmetric warming over the IPWP during the El Niño events in the response of the HC to symmetric and asymmetric SST by removing the effects of SST over the IPWP. The scatterplot of SST versus HC after removing the effects of the IPWP is shown in Fig. 11. The significant relationships between the HEA and SEA, and the HES and SES are not changed after

removing the effects of SST over the IPWP. However, the contrast in the response of HEA to SEA and HES to SES is largely suppressed, and is comparable to that seen over the whole period (Table 1); this result is found consistently in different reanalyses. On the other hand, the response ratio of the HC to SST in the whole period does not appear to be affected by the SST over the IPWP. The result above highlights the role of the equatorially asymmetric SST variations within the

Fig. 11 As in Fig. 6, but after removing the effect of SST over the IPWP



IPWP in contributing to the enhanced response contrast of the HC to SST during the El Niño events.

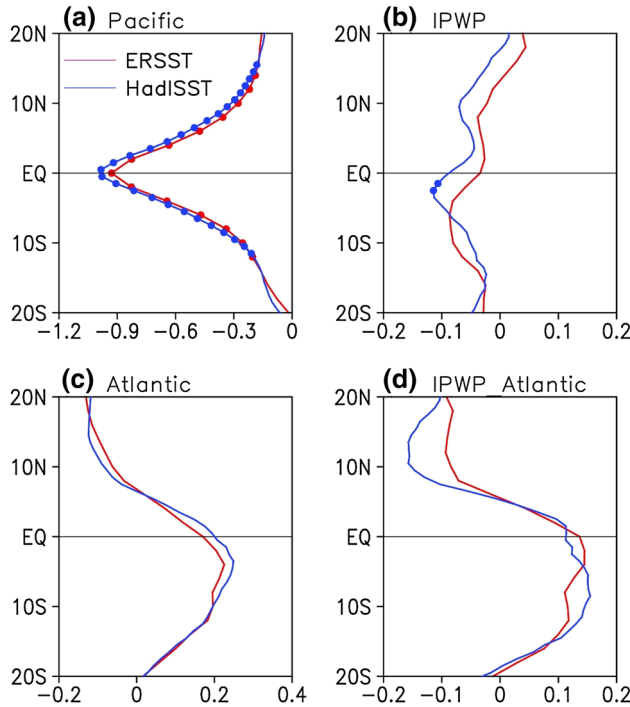
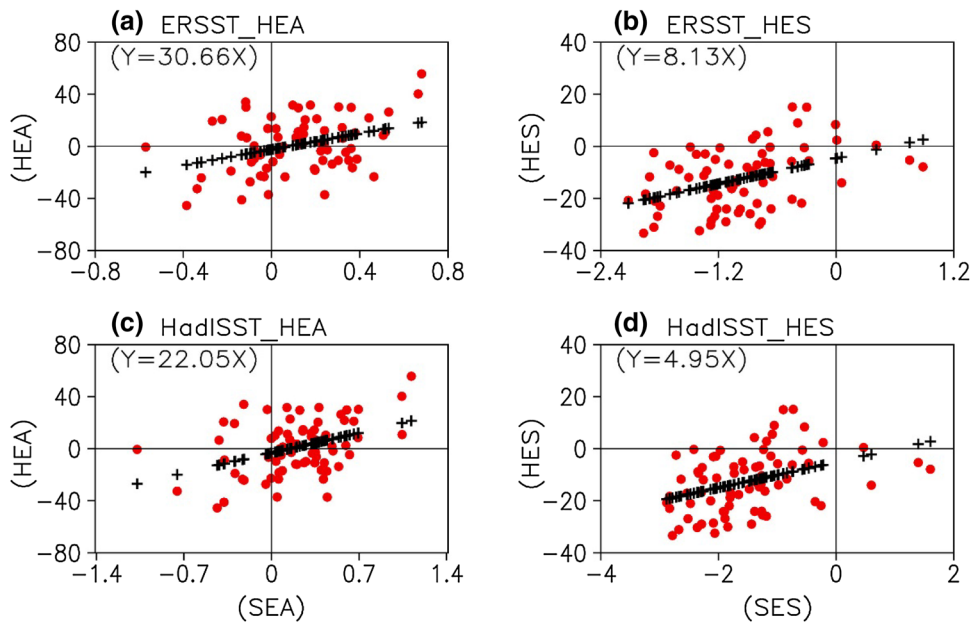


Fig. 12 Profiles of zonal-mean SST anomalies within the tropical **a** Pacific (140°E – 60°W), **b** IPWP (30°E – 140°E), **c** Atlantic (60°W – 30°E), and **d** IPWP and Atlantic (60°W – 140°E) during the La Niña events. Red (blue) lines indicate ERSST (HadISST) data, dotted line indicates significant at the 0.1 level

5 Situation during La Niña events

The response amplitude of the HC to SST during the El Niño events has been analyzed above. However, strong differences between warm and cold ENSO events have been reported (e.g., Feng and Li 2011; Zhang et al. 2015), indicating that the cold events are not simply the opposite of the warm events as reported in many studies (e.g., Feng and Li 2011; Karori et al. 2013; Zhang et al. 2015). The response of the HC to SST during the La Niña events is discussed further in this section. Unlike El Niño events, the explained variances of the EOF1 of HEA and HES during the La Niña events show little change from the result in the whole period; i.e., with values of $\sim 41.6\%$ and $\sim 38.1\%$ using ERAI, respectively (figures not shown). The regional tropical SST profiles over different ocean basins during the La Niña events are presented in Fig. 12. Similar equatorially symmetric but negative SST anomalies are seen over the tropical Pacific. In contrast, unlike El Niño events, insignificant equatorially asymmetric SST anomalies are seen over the IPWP and tropical Atlantic but with opposite signs, being negative over the IPWP but positive over the Atlantic. However, the sum of these SST anomalies is equatorially symmetric, with the maximum around the equator (Fig. 12d). This result is observed in both ERSST

Fig. 13 **a** Scatterplot of the PC1 of the equatorially asymmetric variation of SST (from ERSST) against the PC1 of the equatorially asymmetric variation of the HC (from ERAI) (red dots), and their linear fit (black crosses) during the La Niña events. **b** As in **a**, but for the equatorially symmetric variation of the SST and HC. **c, d** As in **a, b**, but based on the HadISST



and HadISST datasets. Thus, there is no enhancement of the equatorially asymmetric SST anomalies during the La Niña events, which in turn implies that the response contrast of the HC to SST does not vary as much as during the El Niño events. This point is further established by the equivalent response contrast of the HC to SST during the La Niña events and in the whole period; i.e., with response ratio coefficients of 3.8 and 4.5 using ERSST and HadISST, respectively (Fig. 13). Moreover, the EOF1 of the HC during La Niña events is highly consistent with those in the whole period, in both the spatial distribution and explained variance (not shown), indicating the difference between the warm and cold events of ENSO in modulating the response of the HC to tropical SST.

6 Discussion and summary

The impact of ENSO on the response of the HC to different tropical SST meridional structures is investigated using multiple atmospheric and SST datasets over the past four decades. El Niño is associated with equatorially symmetric SST anomalies, which are connected with equatorially symmetric meridional circulation (Lindzen and Nigam 1987; Feng and Li 2013). However, we found that the principal mode of the HC variability (an equatorially asymmetric mode), is strengthened rather than suppressed, with greater explained variance during the El Niño events. Moreover, the response of HEA to SEA and of HES to SES is generally greater during the El Niño events than in the whole period, although there are no obvious changes in the explained variance of the first dominant mode in either the SEA or SES.

By examining the regional SST characteristics during the El Niño events, we found that the anomalous SST over the tropical Pacific and Atlantic are both equatorially symmetric during the El Niño events, but the SST over the IPWP is not. The SST over the southern part of the IPWP shows greater warming than over the northern part, inducing equatorially asymmetric SST anomalies within the IPWP. This asymmetric warming show opposite meridional structure to its climatological distribution: the northern IPWP is warmer than the southern in the climatology, which would increase the variability of SES. After removing the effects of the SST over the IPWP, the enhanced response contrast in El Niño events of the HC to SST is generally suppressed, and is comparable to that seen over the whole period. Moreover, the influence of the tropical Pacific and Atlantic on the response of the HC to different SST meridional structures has been investigated. The response after removing the effects of SST in the corresponding oceans is comparable to the result for the whole study period (not shown), which further establishes that neither the SST over the tropical Pacific nor over the Atlantic contributes to the enhanced response during the El Niño events. This result supports the viewpoint that the inhomogeneous warming of the SST over the IPWP leads to the greater response contrast of the HC to different SST meridional structures, which in turn contributes to the enhanced explained variance of the equatorially asymmetric mode of the HC during the El Niño events.

Moreover, the situation differs between the ENSO warm and cold events; the response contrast of the HC to SST during the La Niña events shows little change from that in the whole period, implying that different physical processes govern the response of HC to SST in El Niño and La Niña

events. The differences between the warm and cold ENSO events mainly derive from the following two points: (1) in the La Niña events the magnitude of SST anomalies over the IPWP is smaller and not as significant as that during the El Niño events; (2) there are equatorially asymmetric SST anomalies during the La Niña events over the tropical Atlantic, but equatorially symmetric anomalies during the El Niño events. The asymmetric SST anomalies over the tropical Atlantic counteract the SST anomalies within the IPWP, resulting in an equatorially symmetric anomalous SST overall during the La Niña events. It is unclear whether oceanic or atmospheric processes are responsible for the different SST meridional structures over the tropical Atlantic in the warm and cold ENSO events. Nor is it known whether the different response contrast is due to internal ocean processes, or to different interaction between the air and sea. In addition, the above results are based on canonical El Niño events, and do not consider the extensively discussed new variant of the El Niño phenomenon, referred to as the Dateline El Niño (Larkin and Harrison 2005), El Niño Modoki (Ashok et al. 2007), Central Pacific El Niño (Yu and Kao 2007), or warm pool El Niño (Kug et al. 2009), whose impacts and evolution differ from those of canonical El Niño events. Moreover, it is reported that central and eastern Pacific El Niño events are associated with different SST meridional distributions (Feng and Li 2013), implying that their impacts on the response of the HC to SST may different. Further investigation of the impacts of this event on the response of the HC to the SST would be of interest, comparing the differences and similarities with those of the canonical events, and exploring the possible mechanisms. Moreover, it is noted that the width of both the HEA and HES has been narrowed during the El Niño events, however, it is still unknown the underlying mechanisms. These questions are still unsolved and will be discussed in our future work.

On the other hand, although the variation of HEA appears to be the main contributor to the enhanced response ratio of the HC to SST during the El Niño events, we have discussed the variation of *Ratio* is discussed rather than of *RegA* (regression coefficient of SES PC1 versus HES PC1). This is due to the following considerations. (1) The definition of *Ratio* is more objective and is not affected by different assimilation systems as both the numerator and denominator contain the variables of circulation and SST. (2) The relationship between the HEA and HES is changeable in different seasons (Feng et al. 2018), but the *Ratio* represents the relative variation of the HC to SST. (3) The standard deviations of SEA and SES in the whole period and during the El Niño events are different (Fig. 9c, d); i.e., the standard deviation of SEA during the whole period is smaller than that during the El Niño events, but the opposite holds for that of the SES. This indicates that the variability of SST in the whole period and during the El Niño events is different, as

is also the case when the effects of the SST over the IPWP (Pacific) are removed, suggesting that a comparison of *RegA* between the whole period and during the El Niño events would not be objective.

In addition, the influence of El Niño on the SST over the Indian Ocean has been discussed extensively (e.g., Lau and Nath 2003; Kumar and Hoerling 2003; Xie et al. 2009), but most research has considered the zonal differences in the SST or taken the Indian Ocean as a whole, with less attention paid to the meridional structures of the SST over this region. In the present study, we have found that the southern part of the IPWP shows greater warming amplitude than the northern part during the El Niño events, particularly in the maturing and decaying phases. It is worth investigating further the possible reasons for this inhomogeneous warming, to compare whether similar warming differences are observed in the central El Niño events, and to examine its associated climatic effects, particularly on the regional meridional circulation. Meanwhile, since the atmosphere–ocean system exhibited strong decadal variability in the late 1970s, and it is reported that the meridional extents of the El Niño and La Niña events show evident decadal variations (Zhang et al. 2009, 2013), it would be interesting to examine whether the decadal variation of the meridional extent influences the meridional structures of the associated SST anomalies, the response of the HC to SST, and the interdecadal variation of the HC. In addition, the role of the background climate conditions in determining the response of the HC to tropical SST deserves further study.

Finally, our results highlight the important impact of the inhomogeneous warming SST over the IPWP on the response contrast of the HC to the SST during the El Niño events, and we find that the response of the meridional circulation during El Niño is at least twice as strong as that in the whole period (~10 vs. ~4). Therefore, the different response of the HC to SST during the El Niño events and in the interannual variations offers a feasible criterion for evaluating the performance of the simulations of the Coupled Model Intercomparison Project (CMIP) models, given that El Niño is the most significant interannual signal in the tropical air–sea system and that its simulation by models has been improved (e.g., Chen et al. 2016, 2017). Further work will investigate the role of El Niño in modulating the responses of the HC to different SST forcing using CMIP outputs by comparing the different response of the HC to SST during El Niño events and in the interannual variations.

Acknowledgements The author Juan Feng acknowledges helpful discussions with Prof. Fred Kucharski and Prof. In-Sik Kang during her visit to the Abdus Salam International Centre for Theoretical Physics (ICTP). This work was jointly supported by the National Natural Science Foundation of China (41790474, 41705131, and 41475076). The HadISST dataset was obtained from the UK Met Office Hadley Centre and is available online at <http://www.metoffice.gov.uk/hadobs/hadisst/>

data.download.html. The NCEP2 and ERSST reanalyses were obtained from NOAA and are available at <http://www.esrl.noaa.gov/psd/data/gridded/>. The ERA-Interim reanalysis was obtained from <http://apps.ecmwf.int/datasets/>. The JRA reanalysis is available online at http://jra.kishou.go.jp/JRA-55/index_en.html.

Open Access This article is distributed under the terms of the Creative Commons Attribution 4.0 International License (<http://creativecommons.org/licenses/by/4.0/>), which permits unrestricted use, distribution, and reproduction in any medium, provided you give appropriate credit to the original author(s) and the source, provide a link to the Creative Commons license, and indicate if changes were made.

References

Ashok K, Behera SK, Rao SA, Weng HY, Yamagata T (2007) El Niño Modoki and its teleconnection. *J Geophys Res Ocean* 112:C11007. <https://doi.org/10.1029/2006JC003798>

Bjerknes J (1969) Atmospheric teleconnections from the equatorial Pacific. *Mon Weather Rev* 97:163–172

Caballero R (2007) Role of eddies in the interannual variability of Hadley cell strength. *Geophys Res Lett* 34:L22705. <https://doi.org/10.1029/2007GL030971>

Cane MA, Zebiak SE (1985) A theory for El Niño and the Southern Oscillation. *Science* 228:1085–1087. <https://doi.org/10.1126/science.228.4703.1085>

Chen L, Yu YQ, Zheng WP (2016) Improved ENSO simulation from climate system model FGOALS-g1.0 to FGOALS-g2. *Clim Dyn* 47:2617–2634. <https://doi.org/10.1007/s00382-016-2988-8>

Chen L, Li T, Yu YQ, Behera SK (2017) A possible explanation for the divergent projection of ENSO amplitude change under global warming. *Clim Dyn* 49:3799–3811. <https://doi.org/10.1007/s00382-017-3544-x>

Dee DP, Uppala SM, Simmons AJ et al (2011) The ERA-Interim reanalysis: configuration and performance of the data assimilation system. *Q J R Meteorol Soc* 137(656):553–597. <https://doi.org/10.1002/qj.828>

DeWeaver E, Nigam S (2004) On the forcing of ENSO teleconnections by anomalous heating and cooling. *J Clim* 17:3225–3235

Dima IM, Wallace JM (2003) On the seasonality of the Hadley cell. *J Atmos Sci* 60:1522–1526

Ebita A, Kobayashi S, Ota Y et al (2011) The Japanese 55-year Reanalysis ‘JRA-55’: an interim report. *SOLA* 7:149–152. <https://doi.org/10.2151/sola.2011-038>

Feng J, Li JP (2011) Influence of El Niño Modoki on spring rainfall over south China. *J Geophys Res Atmo* 116:D13102. <https://doi.org/10.1029/2010JD015160>

Feng J, Li JP (2013) Contrasting impacts of two types of ENSO on the boreal spring Hadley circulation. *J Clim* 26:4773–4789. <https://doi.org/10.1175/JCLI-D-12-00298.1>

Feng R, Li JP, Wang JC (2011) Regime change of the boreal summer Hadley circulation and its connection with the tropical SST. *J Clim* 24:3867–3877. <https://doi.org/10.1175/2011JCLI3959.1>

Feng J, Li JP, Jin FF, Liu ZY, Xing N, Guo YP (2016) Contrasting responses of the Hadley circulation to equatorially asymmetric and symmetric meridional sea surface temperature structures. *J Clim* 29:8949–8963. <https://doi.org/10.1175/JCLI-D-16-0171.1>

Feng J, Li JP, Jin FF, Zhao S, Xie F (2017) The responses of the Hadley circulation to different meridional SST structures in the seasonal cycle. *J Geophys Res Atmos* 122:7785–7799. <https://doi.org/10.1002/2017JD026953>

Feng J, Li JP, Jin FF, Zheng F (2018) A comparison of the response of the Hadley circulation to different tropical SST meridional structures during the equinox seasons. *J Geophys Res Atmos* 123:2591–2604. <https://doi.org/10.1002/2017JD028219>

Fu Q, Johanson CM, Wallace JM, Reichler T (2006) Enhanced mid-latitude tropospheric warming in satellite measurements. *Science* 312:1179

Guan ZY, Xu JJ, Wang PX (1994) Odd and even symmetry of atmospheric circulation-theoretical basis and climatic characteristics. *J Meteorol Res* 8:187–194

Guo YP, Li JP, Feng J, Xie F, Sun C, Zheng JY (2016) The multidecadal variability of the asymmetric mode of the boreal autumn Hadley circulation and its link to the Atlantic Multidecadal Oscillation. *J Clim* 29:5625–5641. <https://doi.org/10.1175/JCLI-D-15-0025.1>

Holton JR (1994) An introduction to dynamic meteorology. Academic Press, New York

Hou AY, Lindzen RS (1992) The influence of concentrated heating on the Hadley circulation. *J Atmos Sci* 49(14):1233–1241

Hu YY, Fu Q (2007) Observed poleward expansion of the Hadley circulation since 1979. *Atmos Chem Phys* 7:5229–5236

Jin FF (1997a) An equatorial ocean recharge paradigm for ENSO. Part I: conceptual model. *J Atmos Sci* 54:811–829. <https://doi.org/10.1175/1520-0469>

Jin FF (1997b) An equatorial ocean recharge paradigm for ENSO. Part II: a stripped-down coupled model. *J Atmos Sci* 54:830–847. <https://doi.org/10.1175/1520-0469>

Kanamitsu M, Ebisuzaki W, Woollen J et al (2002) NCEP-DOE AMIP-II Reanalysis (R-2). *Bull Am Meteorol Soc* 83:1631–1643. <https://doi.org/10.1175/BAMS-83-11-1631>

Karori MA, Li JP, Jin FF (2013) The asymmetric influence of the two types of El Niño and La Niña on summer rainfall over southeast China. *J Clim* 26:4567–4582. <https://doi.org/10.1175/JCLI-D-12-00324.1>

Kiladis GN, Diaz HF (1989) Global climatic anomalies associated with extremes in the Southern Oscillation. *J Clim* 2:1069–1090

Kug JS, Jin FF, An SI (2009) Two types of El Niño events: cold tongue El Niño and warm pool El Niño. *J Clim* 22:1499–1515. <https://doi.org/10.1175/2008JCLI2624.1>

Kumar A, Hoerling MP (2003) The nature and causes for the delayed atmospheric response to El Niño. *J Clim* 16:1391–1403

Larkin NK, Harrison DE (2005) On the definition of El Niño and associated seasonal average U.S. weather anomalies. *Geophys Res Lett* 32:L13705. <https://doi.org/10.1029/2005gl022738>

Latif M, Keenlyside NS (2008) El Niño/Southern Oscillation response to global warming. *PNAS* 106:20578–20583. <https://doi.org/10.1073/pnas.0710860105>

Latif M, Kleeman R, Eckert C (1997) Greenhouse warming, decadal variability, or El Niño? An attempt to understand the anomalous 1990s. *J Clim* 10:2221–2239. [https://doi.org/10.1175/1520-0442\(1997\)010%3c2221:GWDVOE%3e2.0.CO;2](https://doi.org/10.1175/1520-0442(1997)010%3c2221:GWDVOE%3e2.0.CO;2)

Lau NC, Nath MJ (2003) Atmosphere-ocean variations in the Indo-Pacific sector during ENSO episodes. *J Clim* 16:3–20. [https://doi.org/10.1175/1520-0442\(2003\)016%3c0003:AOVITI%3e2.0.CO;2](https://doi.org/10.1175/1520-0442(2003)016%3c0003:AOVITI%3e2.0.CO;2)

Li JP, Feng J (2017) Tropical large-scale atmospheric interaction in association with subtropical aridity trend. In: Fu CB, Mao HT (eds) Aridity trend in Northern China. World Scientific, Singapore

Lindzen RS, Nigam S (1987) On the role of sea surface temperature gradients in forcing low-level winds and convergence in the tropics. *J Atmos Sci* 44:2418–2436. [https://doi.org/10.1175/1520-0469\(1987\)044%3c2418:OTROSS%3e2.0.CO;2](https://doi.org/10.1175/1520-0469(1987)044%3c2418:OTROSS%3e2.0.CO;2)

Lu J, Chen G, Frierson (2008) Response of the zonal mean atmospheric circulation to El Niño versus global warming. *J Clim* 21:5835–5851

Lu J, Deser C, Reichler T (2009) Cause of the widening of the tropical belt since 1958. *Geophys Res Lett* 36(3):L03803. <https://doi.org/10.1029/2008GL036076>

Ma J, Li JP (2008) The principal modes of variability of the boreal winter Hadley cell. *Geophys Res Lett* 35:L01808. <https://doi.org/10.1029/2007GL031883>

Mitas CM, Clement A (2005) Has the Hadley cell been strengthening in recent decades? *Geophys Res Lett* 32:L03809. <https://doi.org/10.1029/2004GL021765>

Mitas CM, Clement A (2006) Recent behaviour of the Hadley cell and tropical thermodynamics in climate models and reanalyses. *Geophys Res Lett* 33:L01810. <https://doi.org/10.1029/2005GL024406>

Nicholls N (1979) A possible method for predicting seasonal tropical cyclone activity in the Australian region. *Mon Weather Rev* 107:1221–1224

Numaguti A (1994) Dynamics and energy balance of the Hadley circulation and the tropical precipitation zones, part II: sensitivity to meridional SST distribution. *J Atmos Sci* 52(8):1128–1141. [https://doi.org/10.1175/1520-0469\(1995\)052%3c1128:DAEBO%3e2.0.CO;2](https://doi.org/10.1175/1520-0469(1995)052%3c1128:DAEBO%3e2.0.CO;2)

Picaut J, Masia F, du Penhoat Y (1997) An advective-reflective conceptual model for the oscillatory nature of the ENSO. *Science* 277:663–666

Rayner NA, Parker DE, Horton EB, Folland CK, Alexander LV, Rowell DP, Kent EC, Kaplan A (2003) Global analyses of sea surface temperature, sea ice, and night marine air temperature since the late nineteenth century. *J Geophys Res Atmos* 104(D14):4407. <https://doi.org/10.1029/2002JD002670>

Rind D, Rossow WB (1984) The effects of physical processes on the Hadley circulation. *J Atmos Sci* 41(4):479–507. [https://doi.org/10.1175/1520-0469\(1984\)041%3c0479:TEOPP%3e2.0.CO;2](https://doi.org/10.1175/1520-0469(1984)041%3c0479:TEOPP%3e2.0.CO;2)

Schneider E, Lindzen RS (1977) Axially symmetric steady state models of the basic state of instability and climate studies. Part I: linearized calculations. *J Atmos Sci* 34:253–279. [https://doi.org/10.1175/1520-0469\(1977\)034%3c0263:ASSSM%3e2.0.CO;2](https://doi.org/10.1175/1520-0469(1977)034%3c0263:ASSSM%3e2.0.CO;2)

Seager R, Harnik N, Kushnir Y, Robinson W, Miller J (2003) Mechanisms of hemispherically symmetric climate variability. *J Clim* 16:2960–2978. [https://doi.org/10.1175/1520-0442\(2003\)016%3c2960:MOHSCV%3e2.0.CO;2](https://doi.org/10.1175/1520-0442(2003)016%3c2960:MOHSCV%3e2.0.CO;2)

Smith TM, Reynolds RW, Peterson TC, Lawrimore J (2008) Improvements to NOAA's historical merged land-ocean surface temperature analysis (1880–2006). *J Clim* 21:2283–2296. <https://doi.org/10.1175/2007JCLI2100.1>

Stachnik JP, Schumacher C (2011) A comparison of the Hadley circulation in modern reanalyses. *J Geophys Res Atmos* 116:D22102. <https://doi.org/10.1029/2011JD016677>

Sun Y, Zhou TJ (2014) How does El Niño affect the interannual variability of the boreal summer Hadley Circulation? *J Clim* 27:2622–2642. <https://doi.org/10.1175/JCLI-D-13-00277.1>

Tomita T, Yasunari T (1996) Role of the northeast winter monsoon on the biennial oscillation of the ENSO/monsoon system. *J Meteorol Soc Jpn* 74:399–413

Wang PX, Guan ZY, Xu JJ (1994) Odd and even symmetry of atmospheric circulation—part II: measurement and anomaly analysis. *J Meteorol Res* 8:365–371

Wang C, Weisberg RH, Virmani JI (1999) Western Pacific interannual variability associated with the El Niño Southern Oscillation. *J Geophys Res: Oceans* 104(C3):5131–5149

Wang B, Wu RG, Fu XH (2000) Pacific-East Asian teleconnection: how does ENSO affect East Asian Climate? *J Clim* 13:1517–1536. [https://doi.org/10.1175/1520-0442\(2000\)013%3c1517:PEATH%3e2.0.CO;2](https://doi.org/10.1175/1520-0442(2000)013%3c1517:PEATH%3e2.0.CO;2)

Xie SP, Hu KM, Hafner J, Tokinaga H, Du Y, Huang G, Sampe T (2009) Indian ocean capacitor effect on Indo-Western Pacific climate during the summer following El Niño. *J Clim* 22:730–747. <https://doi.org/10.1175/2008JCLI2544.1>

Yu JY, Kao HY (2007) Decadal changes of ENSO persistence barrier in SST and ocean heat content indices: 1958–2001. *J Geophys Res* 112:D13106. <https://doi.org/10.1029/2006JD007654>

Zhang Y, Wallace JM, Battisti DS (1997) ENSO-like interdecadal variability: 1900–93. *J Clim* 10:1004–1020. [https://doi.org/10.1175/1520-0442\(1997\)010%3c1004:ELIV%3e2.0.CO;2](https://doi.org/10.1175/1520-0442(1997)010%3c1004:ELIV%3e2.0.CO;2)

Zhang WJ, Li JP, Jin FF (2009) Spatial and temporal features of ENSO meridional scales. *Geophys Res Lett* 36:L15605. <https://doi.org/10.1029/2009GL038672>

Zhang WJ, Jin FF, Zhao JX, Li JP (2013) On the Bias in Simulated ENSO SSTA meridional widths of CMIP3 models. *J Clim* 26:3173–3186. <https://doi.org/10.1175/JCLI-D-12-00347.1>

Zhang WJ, Wang L, Xiang BQ, Qi L, He JH (2015) Impacts of two types of La Niña on the NAO during boreal winter. *Clim Dyn* 44:1351–1366. <https://doi.org/10.1007/s00382-014-2155-z>

Publisher's Note Springer Nature remains neutral with regard to jurisdictional claims in published maps and institutional affiliations.